S100A4 influences cancer stem cell-like properties of MGC803 gastric cancer cells by regulating *GDF15* expression

JUNFU GUO[1,2], YUE BIAN[1], YU WANG[1], LISHA CHEN[1], AIWEN YU[1,3] and XIUJU SUN[1]

[1]Department of Medical Genetics, China Medical University, Shenyang, Liaoning 110122; [2]Teaching and Experiment Center, Liaoning University of Traditional Chinese Medicine, Shenyang, Liaoning 110847; [3]Department of Rehabilitation, The First Affiliated Hospital of China Medical University, Shenyang, Liaoning 110001, P.R. China

Received March 7, 2016; Accepted April 19, 2016

DOI: 10.3892/ijo.2016.3556

Abstract. Many studies have revealed that *S100A4* is involved in cancer progression by affecting a variety of biological functions. Our previous study showed that *S100A4* influences many biological properties of gastric cancer cells; however, the underlying mechanisms are far from clear. In this study, we used cDNA microarray analysis to investigate the global alterations in gene expression in MGC803 gastric cancer cells after siRNA-mediated *S100A4* inhibition. Among the total genes investigated, 179 differentially expressed genes (38 upregulated and 141 downregulated) were detected in *S100A4*-siRNA transfected MGC803 cells compared with NC-siRNA transfected cells. We focused on the *GDF15* gene, which was significantly downregulated after *S100A4* inhibition. ChIP studies showed that the S100A4 protein binds to the *GDF15* promoter, implicating S100A4 in *GDF15* regulation at the transcriptional level. *GDF15* overexpression promoted CSC-like properties of MGC803 cells, such as spheroid and soft-agar colony forming abilities. *S100A4* inhibition suppressed the CSC-like properties of the cells, whereas, GV141-*GDF15* vector transfection reversed these effects. Our results suggest that *S100A4* influences the CSC-like properties of MGC803 gastric cancer cells by regulating *GDF15* expression.

Introduction

S100A4 (also known as calvasculin), belongs to the S100 family of Ca^{2+}-binding proteins. The human *S100A4* gene is located in chromosome 1q21. The S100A4 protein occurs as non-covalently bound homodimers with the ability to interact with an array of target proteins in a calcium-dependent manner (1). S100A4 overexpression has been reported in several types of cancer and is associated with invasion and metastasis and poor patient prognosis (2-4). Many studies have confirmed that *S100A4* is involved in a variety of biological effects. Knockdown of *S100A4* inhibited the invasiveness of esophageal squamous cell carcinoma cells, with elevated *E-cadherin* expression (5). The siRNA-mediated silencing of *S100A4* downregulated *MMP-13* expression and suppressed breast cancer cell migration and angiogenesis (6). Recently, increased expression of P27 and cleaved caspase-3 has been reported in S100A4-deficient pancreatic tumors, while cyclin E expression was found to be decreased. S100A4-deficient tumors have reduced expression of vascular endothelial growth factor (VEGF), suggesting reduced angiogenesis (7). Our group previously showed that *S100A4* inhibition mediated by RNA interference (RNAi) led to reduced proliferation and increased apoptosis of BGC823 gastric cancer cells. Intratumoral injection of p*S100A4*-shRNA suppressed tumor growth in nude mice. We also found that *S100A4* inhibition decreased expression of both *NF-κB p65* and phosphorylated *(Ser32)-I-κB-α* in BGC823 cells (8). These studies indicate that *S100A4* exerts its function by affecting downstream gene expression although the mechanisms remain to be fully clarified.

Accumulating evidence suggests that cancer-initiating cells (CIC) or cancer stem cells (CSC) are a rare subpopulation of cells with self-renewal capacity (9,10) and are responsible for cancer initiation, progression, metastasis, relapse, radioresistance and chemoresistance (11-13). *S100A4* knockdown in head and neck CICs reduced their stemness properties both *in vitro* and *in vivo* (14). Our previous study showed that S100A4 mediated the effects of IL-1β on the CSC-like properties of MGC803 gastric cancer cells (unpublished data); however, the mechanisms underlying this effect are far from clear. In this study, we investigated the hypothesis that *S100A4* affects the CSC-like properties of MGC803 gastric cancer cells via regulation of downstream gene expression.

In this study, cDNA microarray analysis showed differential expression of 179 of the total genes after siRNA-mediated *S100A4* knockdown in MGC803 gastric cancer cells. We then focused specifically on the *GDF15* gene, which was significantly downregulated after *S100A4* inhibition. ChIP assays showed that S100A4 protein binds to the *GDF15* promoter, indicating that S100A4 may participate in the transcriptional

Correspondence to: Professor Xiuju Sun, Department of Medical Genetics, China Medical University, 77 Puhe Road, Shenyang North New Area, Shenyang, Liaoning 110122, P.R. China
E-mail: xjsun@mail.cmu.edu.cn

Key words: gastric cancer, *S100A4*, *GDF15*, spheroid, soft-agar colony

regulation of *GDF15*. *GDF15* overexpression promoted the CSC-like properties of MGC803 cells, such as spheroid and soft-agar colony forming abilities. Finally, rescue experiments indicated that *S100A4* influences the CSC-like properties of MGC803 gastric cancer cells by regulating *GDF15* expression.

Materials and methods

Cell culture. The human gastric cancer cell line MGC803 was purchased from the Cell Resource Center, Institute of Basic Medical Sciences (IBMS), Chinese Academy of Medical Sciences and Peking Union Medical College (CAMS/PUMC). Cells were cultured in RPMI-1640 medium (Invitrogen, Carlsbad, CA, USA) supplemented with 10% fetal bovine serum at 37˚C in a humidified incubator containing 5% CO_2.

Transfection of S100A4-specific small interfering RNA (siRNA). Duplex siRNA oligos specific for human *S100A4* were synthesized by GenePharma (Shanghai, China). The siRNA sequences were as follows: 5'-GCAUCGCCAUGAUGUGUA ATT-3', and 5'-UUACACAUCAUGGCGAUGCTT-3'. Negative control (NC) siRNAs were provided by GenePharma. MGC803 cells were transfected with 20 nM of siRNA using Lipofectamine™ 2000 transfection reagent (Invitrogen) according to the manufacturer's instuctions. The cells transfected with *S100A4*-siRNA or NC-siRNA were referred to as MGC803/*S100A4*-siRNA cells or MGC803/NC-siRNA cells, respectively. Cells were harvested at 48 h after transfection for use in the subsequent associated experiments.

Table I. The primers used for qPCR analysis.

Gene	Primer sequence (5'-3')
S100A4	F: CCCTGGATGTGATGGTGT
	R: GTTGTCCCTGTTGCTGTC
PLK2	F: GAGCAGCTGAGCACATCATT
	R: CATGTGAGCACCATTGTTGA
MDM2	F: GTGAAGGAAACTGGGGAGTCTT
	R: AGGTACAGACATTTTGGTATTGCA
MT1G	F: CTTCTCGCTTGGGAACTCTA
	R: AGGGGTCAAGATTGTAGCAAA
TSP-1	F: CGGAAAGAGTTTAAGTGTCTAACAAA
	R: TCCTTATTGGGAATACTTCTCTGC
STMN3	F: GTCCCACAAAAGCCAGATGT
	R: ACCAAGACAGCCCCAGAAG
GDF15	F: CTCCAGATTCCGAGAGTTGC
	R: AGAGATACGCAGGTGCAGGT
GDF15 promoter	F: AGCTGTGGTCATTGGAGTGTT
	R: TTCACCGTCCTGAGTTCTTGC
GAPDH	F: ATCATCAGCAATGCCTCC
	R: CATCACGCCACAGTTTCC

F, forward; R, reverse.

RNA extraction and quantitative reverse transcription polymerase chain reaction (qRT-PCR). Total cellular RNA was extracted using TRIzol reagent (Invitrogen). Reverse transcription reaction was performed using the First-Strand cDNA synthesis kit (Promega, Madison, WI, USA) with 1 μg of RNA in a final volume of 20 μl. The newly synthesized cDNA was amplified by quantitative PCR and PCR analysis was carried out using SYBR Premix Ex TaqII (Takara Biotechnology, Tokyo, Japan). Reactions were processed and analyzed on an ABI 7500 Real-time PCR system (Applied Biosystems, Carlsbad, CA, USA). The PCR conditions were 30 sec at 95˚C followed by 45 cycles of 95˚C for 5 sec and 60˚C for 34 sec. All of the quantitative PCR reactions were run in triplicate, and data were analyzed according to the comparative Ct ($2^{-\Delta\Delta Ct}$) method. The qPCR primers (Table I) were synthesized by Sangon Biotech (Shanghai, China). Experiments were carried out independently three times.

Western blot analysis. Whole cell extracts were prepared by homogenizing cells in a lysis buffer [50 mM Tris (pH 7.2), 500 mM NaCl, 1% Triton X-100, 0.5% sodium deoxycholate, 0.1% SDS, 10 mM $MgCl_2$ with 10 μg/ml leupeptin, 10 μg/ml aprotinin, and 1 mM PMSF]. Protein lysates were quantified by the Bradford method. Proteins were separated by sodium-dodecyl sulfate polyacrylamide gel (12%) electrophoresis, transferred onto PVDF membranes (Millipore, Bedford, MA, USA) and blocked with TBST supplemented with 5% non-fat milk. The membranes were immunoblotted with primary antibodies: rabbit anti-S100A4 antibody (1:500 dilution; Abcam); rabbit anti-GDF15 antibody (1:1,000 dilution; ImmunoWay); and rabbit anti-β-actin antibody (1:500 dilution; Santa Cruz). After washing, membranes were incubated with a peroxidase-conjugated second antibody: mouse anti-rabbit IgG for S100A4 or GDF15 and β-actin. Immunoreactivity was detected using an enhanced chemiluminescence reagent (Amersham Biosciences, Freiburg, Germany) and visualized with Micro Chemi (DNR Bio-Imaging Systems, Jerusalem, Israel). Experiments were carried out independently three times.

Microarray analysis. Total RNA from the MGC803/*S100A4*-siRNA cells or MGC803/NC-siRNA cells was extracted, cleaned up, reverse-transcribed, and hybridized to the Genechip® PrimeView™ Human Gene Expression array (Affymetrix, Santa Clara, CA, USA) by the GeneChem Co. (Shanghai, China). Fold changes in expression and P-values were calculated from the raw data. Genes showing significant differential expression were defined as those exhibiting changes in expression exceeding 1.5-fold with a P-value of <0.05; the differentially expressed gene transcripts were then included in further analyses. Briefly, gene transcripts showing significant changes in expression in the transcriptome array analysis were mapped to their corresponding Kyoto Encyclopedia of Genes and Genomes (KEGG) pathways and Gene Ontology (GO) molecular functions.

Chromatin immunoprecipitation (ChIP) assay. ChIP assays were performed using ChIP-IT® Express Enzymatic kits (Active Motif) according to the manufacturer's instructions. Briefly, ~$4.5x10^7$ MGC803 cells were cross-linked with

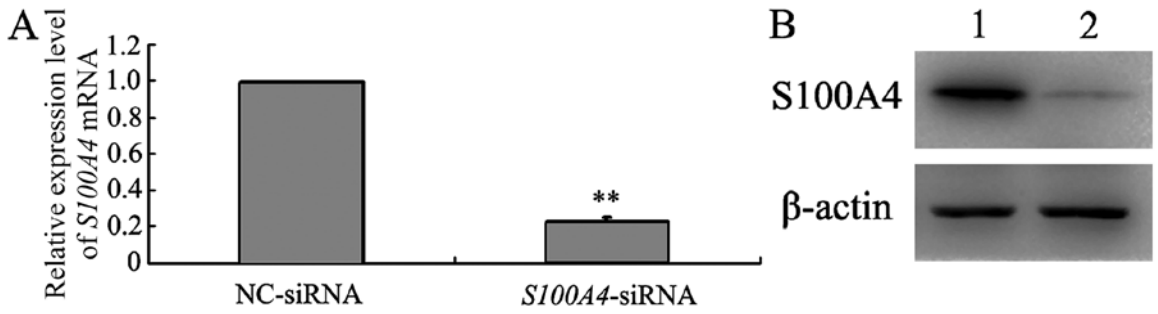

Figure 1. Downregulation of *S100A4* expression in gastric cancer cells by RNAi. MGC803 cells transfected with either *S100A4*-siRNA or NC-siRNA were grown under normal culture conditions. mRNA and protein were extracted for qRT-PCR (A) and western blot (B) analyses, respectively, as described in Materials and methods. (A) Data represent the mean ± SD from three experiments (**P<0.01). (B) Lanes 1 and 2, MGC803/NC-siRNA cells and MGC803/*S100A4*-siRNA cells, respectively, at 48 h after transfection.

60 ml 1% formaldehyde for 10 min at 37˚C. The cells were then resuspended in 3 ml lysis buffer containing 15 µl PIC and 15 µl PMSF and incubated for 45 min on ice. Fragments (150-450 bp) were generated by enzymatic shearing. The recovered supernatant (400 µl) was incubated with 10 µg anti-S100A4 antibody (Abcam) or 10 µg normal isotype control IgG and 25 µl magnetic beads overnight at 4˚C with rotation. Approximately 200 µl of the recovered supernatant was used as the input. After washing the magnetic beads/antibody/DNA complex, crosslinking was reversed by incubation with 10 µl 5 M NaCl at 65˚C for 8 h. The DNA samples were then purified and analyzed by quantitative polymerase chain reaction (qPCR) using the primers listed in Table I. Experiments were carried out independently three times.

Construction and transfection of the GDF15 expression vector. GV141-*GDF15*, the expression vector specific for human *GDF15* was constructed by GeneChem. GV141-empty (negative control) was provided by GeneChem. MGC803 cells were transfected with these vectors using Lipofectamine™ 2000 transfection reagent (Invitrogen) according to the manufacturer's instructions. The cells transfected with GV141-*GDF15* or GV141-empty were referred to as MGC803/GV141-*GDF15* cells or MGC803/GV141-empty cells, respectively. Cells were harvested at 48 h after transfection for the associated experiments.

Spheroid formation assay. Single cell suspensions of transfected MGC803 cells were plated ($1x10^3$ cells/well) in 24-well Ultra-Low Attachment Plates (Corning) and maintained in serum-free DMEM/F-12 medium supplemented with 20 ng/ml basic fibroblast growth factor, 20 ng/ml epidermal growth factor, 10 mmol/l HEPES, 0.4% bovine serum albumin and B27 supplement (1:50 dilution; Invitrogen) for 7 days. The number of spheroids (diameter >75 µm) was counted and representative images were captured under an inverted microscope (Olympus, Tokyo, Japan). Experiments were carried out independently three times.

Soft-agar colony formation assay. Single cell suspensions of transfected MGC803 cells were plated into 6-well plates ($3x10^3$ cells/well) in RPMI-1640 (Invitrogen) containing 10% FBS and 0.3% low melting-point agarose (Amresco, Solon, OH, USA) on a base layer of 0.5% low melting-point agarose. After incubation for 7 days at 37˚C, the number of colonies >50 µm was counted and photographed. Experiments were carried out independently three times.

Rescue assay after co-transfection of S100A4-siRNA and GV141-GDF15. S100A4-siRNA and the GV141-*GDF15* vector were co-transfected into MGC803 cells using Lipofectamine™ 2000 (Invitrogen) to generate MGC803/*S100A4*-siRNA+ GV141-*GDF15* cells. *S100A4*-siRNA and GV141-empty vector were co-transfected to generate MGC803/*S100A4*-siRNA+ GV141-empty cells as a control. At 48 h after transfection, cells were harvested for investigation of CSC-like properties by spheroid formation assays and soft-agar colony formation assays. Experiments were carried out independently three times.

Statistical analysis. Statistical analysis was carried out by Student's t-test using the Statistical Package for the Social Sciences (SPSS Inc., Chicago, IL, USA), where P<0.05 was considered to indicate statistical significance.

Results

Knockdown of S100A4 expression in MGC803 cells by RNA interference (RNAi). The effect of *S100A4*-siRNA transfection on *S100A4* gene silencing was evaluated by both qRT-PCR and western blot analyses. As shown in Fig. 1, endogenous *S100A4* mRNA and protein levels were reduced in MGC803/*S100A4*-siRNA cells at 48 h post-transfection compared with those in MGC803/NC-siRNA cells. There was no significant difference in β-actin expression between the two groups. These data indicate that *S100A4*-siRNA effectively suppressed *S100A4* expression in MGC803 cells.

Gene expression profiling in MGC803 cells after S100A4 silencing. Alterations in the expression of the MGC803 cell transcriptome associated with *S100A4* knockdown were analyzed by cDNA microarray profiling. Compared with the profile of MGC803/NC-siRNA cells, differential expression of 179 transcripts was identified in MGC803/*S100A4*-siRNA cells (>1.5-fold change in expression; P<0.05) (Fig. 2). Of the 179 differentially expressed genes (DEGs), 38 were upregulated and 141 were downregulated in *S100A4*-silenced cells (data not shown in detail).

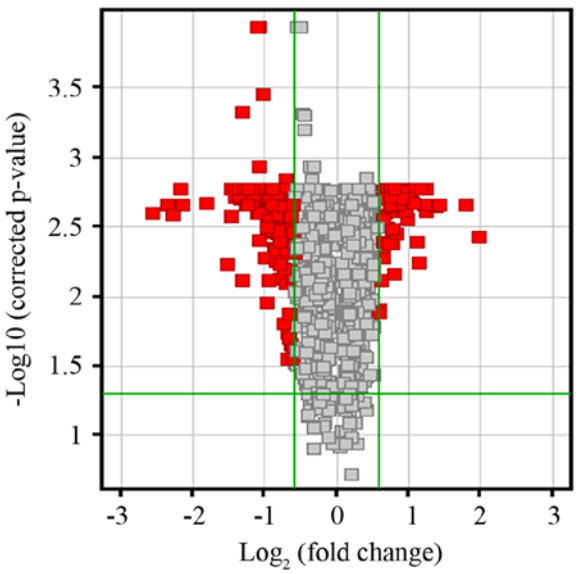

Figure 2. Volcano plot analysis of differentially expressed genes identified in cDNA microarray analysis. The expression of 179 genes was significantly changed (>1.5-fold) in MGC803/*S100A4*-siRNA cells at 48 h after transfection compared to the MGC803/NC-siRNA cells (P<0.05). A total of 38 genes were upregulated and 141 were downregulated. x-axis parallel lines, P-value, 0.05. y-axis parallel lines, fold change = 1.5. Red areas indicate significant changes in gene expression.

Table II. Functional enrichment of GO analysis following *S100A4* knockdown in gastric cancer cells.

Molecular function
Transferase activity
Kinase activity
Receptor binding
Actin filament binding
Hydrogen ion transmembrane transporter activity
Enzyme regulator activity
Phosphotransferase activity
Receptor activity
Monovalent inorganic cation transmembrane transporter activity
Protease inhibitor activity

Table III. Functional enrichment of KEGG pathway analysis following *S100A4* knockdown in gastric cancer cells.

KEGG pathway
p53 signaling pathway
Bladder cancer
Glutathione metabolism
CCR5 pathway
Focal adhesion
Complement and coagulation cascades
ECM receptor interaction
Prostate cancer
Vasopressin regulated water reabsorption
SARS pathway

Gene ontology term and KEGG pathway enrichment analyses. The molecular functions involving DEGs were identified by Gene Ontology (GO) enrichment analysis. In total, 10 GO terms were identified (Table II). To identify well-characterized pathways that were significantly represented, the list of genes was also subjected to Kyoto Encyclopedia of Genes and Genomes (KEGG) pathway analysis. Ten significantly enriched pathways were identified (Table III), although the vast majority of the 179 DEGs could not be assigned to these signaling pathways or molecular classifications.

Validation of microarray data by qRT-PCR analysis. The microarray data were validated by qRT-PCR analysis of RNA from the same cell samples. As shown in Fig. 3, the expression profiles of the six genes selected from the 179 DEGs were consistent with those determined in the microarray analysis; thus, validating the accuracy of the microarray data. Among the DEGs, expression of the growth differentiation factor-15 gene (*GDF15*) was shown to be downregulated by 5.11- and 8.18-fold by microarray and qRT-PCR analyses, respectively. Thus, *GDF15* was identified as one of the most downregulated genes in MGC803 cells following *S100A4* inhibition using both these techniques.

GDF15 is an important downstream gene of S100A4. GDF15 protein expression in MGC803 cells after *S100A4* inhibition

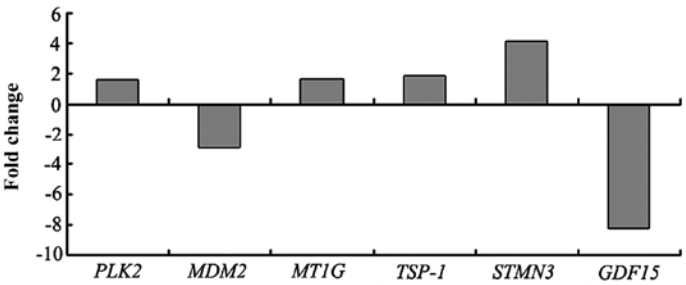

qRT-PCR	1.58	-2.85	1.66	1.84	4.15	-8.18
Microarray Analysis	1.87	-1.55	3.46	2.31	3.95	-5.11

Figure 3. Validation of microarray data by qRT-PCR. The expression of six differentially expressed genes identified in microarray analysis was detected by qRT-PCR. Data represent the mean of three experiments, normalized to *GAPDH*, and presented as fold change in expression in MGC803/*S100A4*-siRNA cells relative to that in MGC803/NC-siRNA cells.

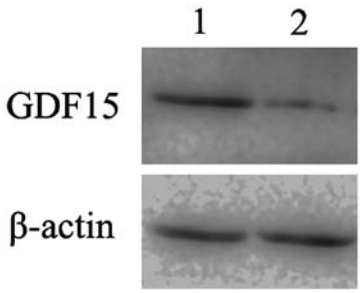

Figure 4. The effect of *S100A4* inhibition on GDF15 protein expression. GDF15 protein levels were detected by western blot analysis after *S100A4* inhibition. Lanes 1 and 2, MGC803/NC-siRNA cells and MGC803/*S100A4*-siRNA cells, respectively, at 48 h after transfection.

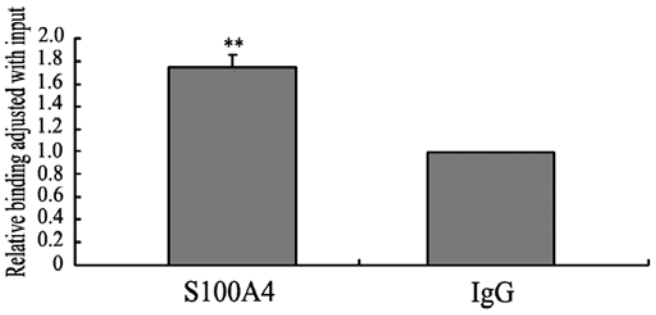

Figure 5. ChIP assays indicated that *S100A4* binds to the *GDF15* promoter *in vivo*. ChIP assays were performed in MGC803 cells using an antibody directed against *S100A4* or an IgG control. ChIP-derived DNA was amplified by qPCR with specific primers designed to amplify the proximal promoter region (-113 bp to +61) of *GDF15*. Data are shown relative to qPCR products amplified with input DNA. Data represent the mean ± SD from three experiments (**P<0.01).

was also determined by western blot analysis. *S100A4*-siRNA transfection induced a substantial decrease in GDF15 protein expression in MGC803 cells (Fig. 4), further confirming that *GDF15* is an important downstream gene of *S100A4* and subject to positive regulation.

ChIP analysis of S100A4 binding to the GDF15 promoter. To determine whether S100A4 binds to the *GDF15* promoter *in vivo*, we performed chromatin immunoprecipitation (ChIP) and then analyzed the quantity of DNA fragments flanking the proximal promoter region (-113 to +61 bp) of *GDF15* by qPCR. The qPCR analysis showed that the quantity of DNA fragments derived from immunoprecipitation with the anti-S100A4 antibody was almost 1.7-fold higher than that derived from immunoprecipitation with the IgG antibody (Fig. 5). These results suggested that S100A4 might bind to the *GDF15* promoter *in vivo*, and therefore implicates S100A4 in the regulation of *GDF15* expression at the transcriptional level.

GDF15 overexpression promotes the CSC-like properties of MGC803 cells. Compared with GV141-empty vector transfection, GV141-*GDF15* transfection into MGC803 cells led to increased *GDF15* expression at both the mRNA and protein levels (Fig. 6). We then investigated the effects of *GDF15* on the CSC-like properties of MGC803 cells by performing spheroid formation and soft-agar colony formation assays. More spheroids and colonies were observed in MGC803/GV141-*GDF15* cells than in MGC803/GV141-empty cells (Fig. 7), suggesting that *GDF15* overexpression promotes the CSC-like properties of MGC803 cells.

GDF15 mediates the effects of S100A4 on CSC-like properties of MGC803 cells. We first explored the effects of *S100A4* inhibition on CSC-like properties of MGC803 cells. MGC803/*S100A4*-siRNA cells formed fewer spheroids and colonies than MGC803/NC-siRNA cells, which suggested that *S100A4* inhibition decreased the CSC-like properties of MGC803 cells (Fig. 8). To corroborate the role of *GDF15* in *S100A4*-regulated CSC-like properties, we carried out rescue experiments by co-transfection of *S100A4*-siRNA with GV141-*GDF15* or GV141-empty into MGC803 cells. qRT-PCR and western blot analyses showed that compared to MGC803/*S100A4*-siRNA+GV141-empty cells, MGC803/*S100A4*-siRNA+GV141-GDF15 cells displayed increased expression of *GDF15* at 48 h after transfection. This indicated that the GV141-*GDF15* vector transfection reversed the downregulation of *GDF15* caused by *S100A4* inhibition (Fig. 9). Furthermore, compared with MGC803/*S100A4*-siRNA+GV14-empty cells,

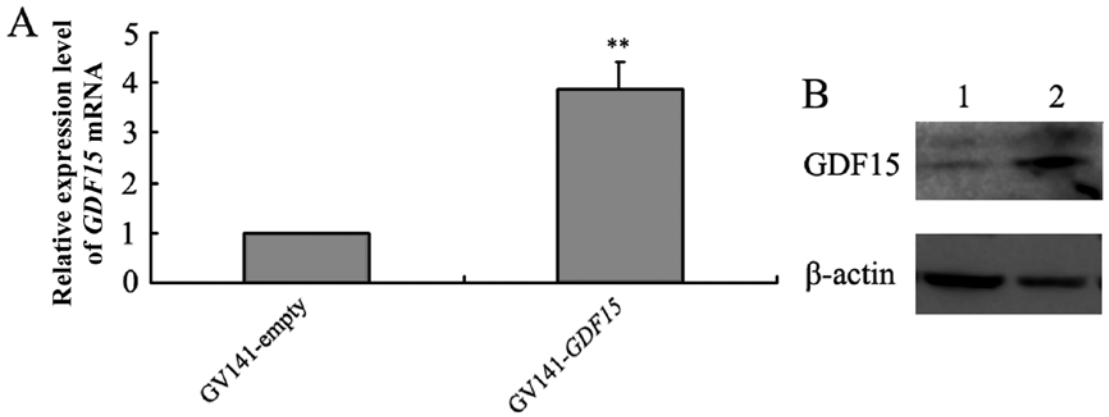

Figure 6. GV141-*GDF15* transfection enhances *GDF15* expression in MGC803 cells. Expression of *GDF15* in MGC803/GV141-*GDF15* cells or MGC803/GV141-empty cells was analyzed by qRT-PCR (A) and western blotting (B), respectively, as described in Materials and methods. (A) Data represent the mean ± SD from three experiments (**P<0.01). (B) Lanes 1 and 2, GV141-empty vector and GV141-*GDF15* transfection, respectively, at 48 h after transfection.

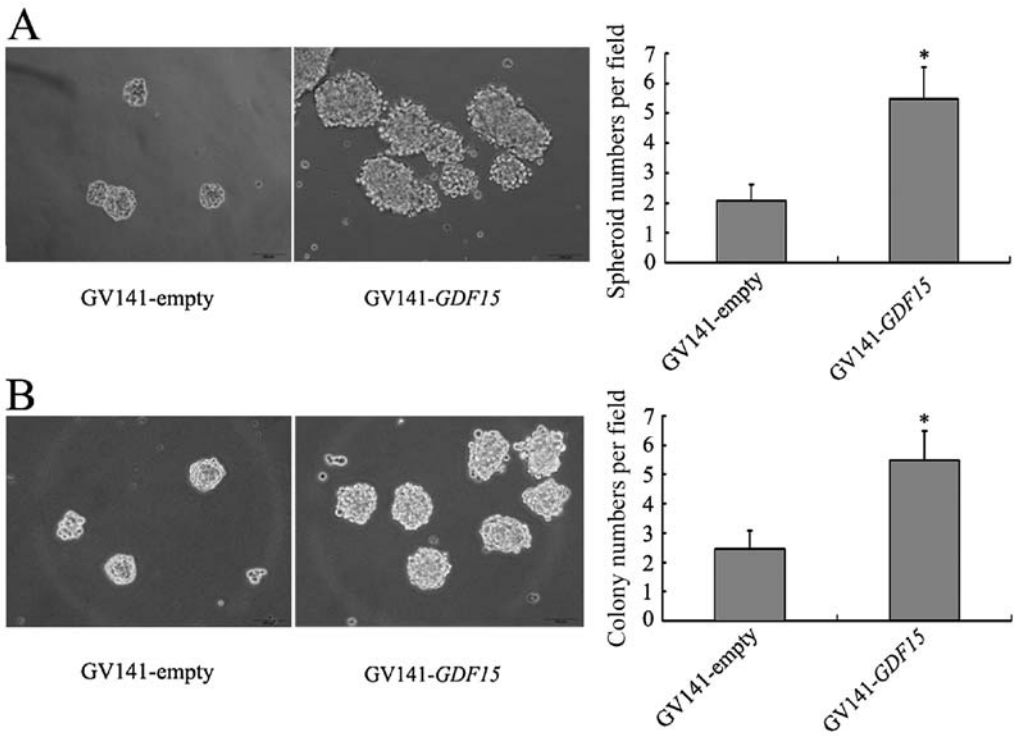

Figure 7. The effects of *GDF15* on the CSC-like properties of MGC803 cells. (A) Representative images of spheroids formed by MGC803/GV141-empty or MGC803/GV141-*GDF15* cells (left, magnification, x20). Bar graph (right) represents the mean number of spheroids from five randomly selected fields under the microscope, and error bars represent SD, *P<0.05. (B) Representative images of colonies formed in soft-agar by MGC803/GV141-empty or MGC803/GV141-*GDF15* cells (left, magnification, x20). Bar graph (right) represents the mean number of colonies from five randomly selected fields under the microscope, and error bars represent SD, *P<0.05. All the results were obtained from three experiments.

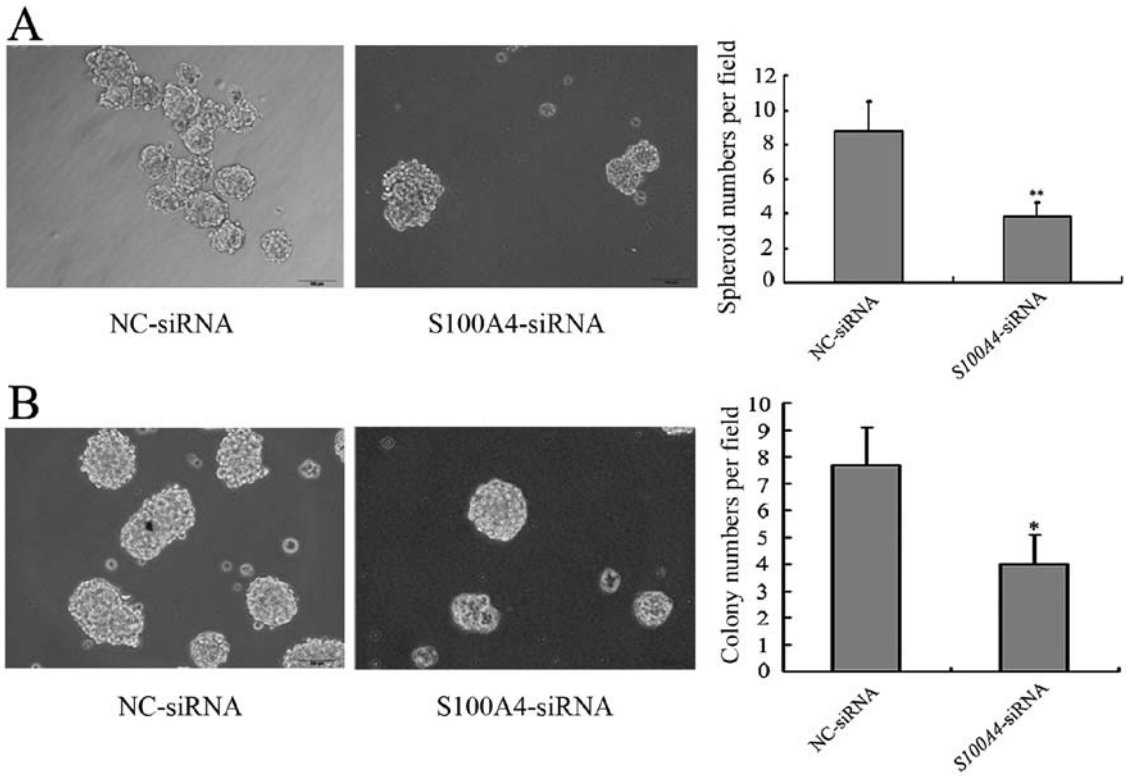

Figure 8. *S100A4*-siRNA transfection inhibits the spheroid and soft-agar colony forming abilities of MGC803 cells. (A) Detection of spheroid forming ability: representative images of spheroids formed by MGC803/NC-siRNA or MGC803/*S100A4*-siRNA cells (left, magnification, x20). Bar graph (right) represents the mean number of spheroids from five randomly selected fields under the microscope, and error bars represent SD, **P<0.01. (B) Detection of colony forming ability: representative images of colonies formed by MGC803/NC-siRNA or MGC803/*S100A4*-siRNA cells (left, magnification, x20). Bar graph (right) represents the mean number of colonies from five randomly selected fields under the microscope, and error bars represent SD, *P<0.05. All the results were obtained from three experiments.

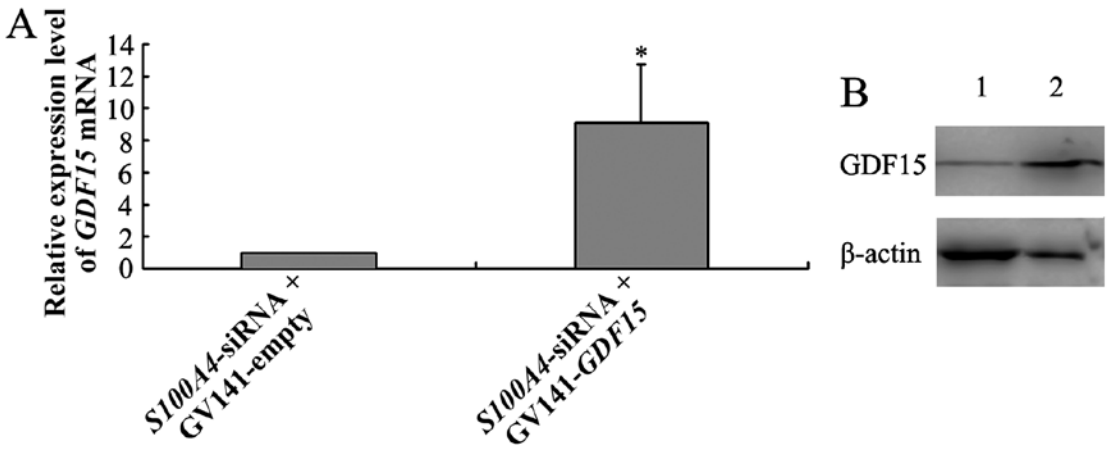

Figure 9. GV141-*GDF15* vector transfection reverses the downregulation of *GDF15* by *S100A4* inhibition. MGC803 cells were co-transfected with *S100A4*-siRNA and either GV141-empty vector or GV141-*GDF15* vector. *GDF15* expression in the co-transfected cells was analyzed by qRT-PCR (A) and western blotting (B), respectively, as described in Materials and methods. (A) Data represent the mean ± SD from three experiments (*P<0.05). (B) Lanes 1 and 2, expression of GDF15 in MGC803 cells at 48 h after co-transfection of *S100A4*-siRNA with either GV141-empty vector or GV141-*GDF15* vector, respectively.

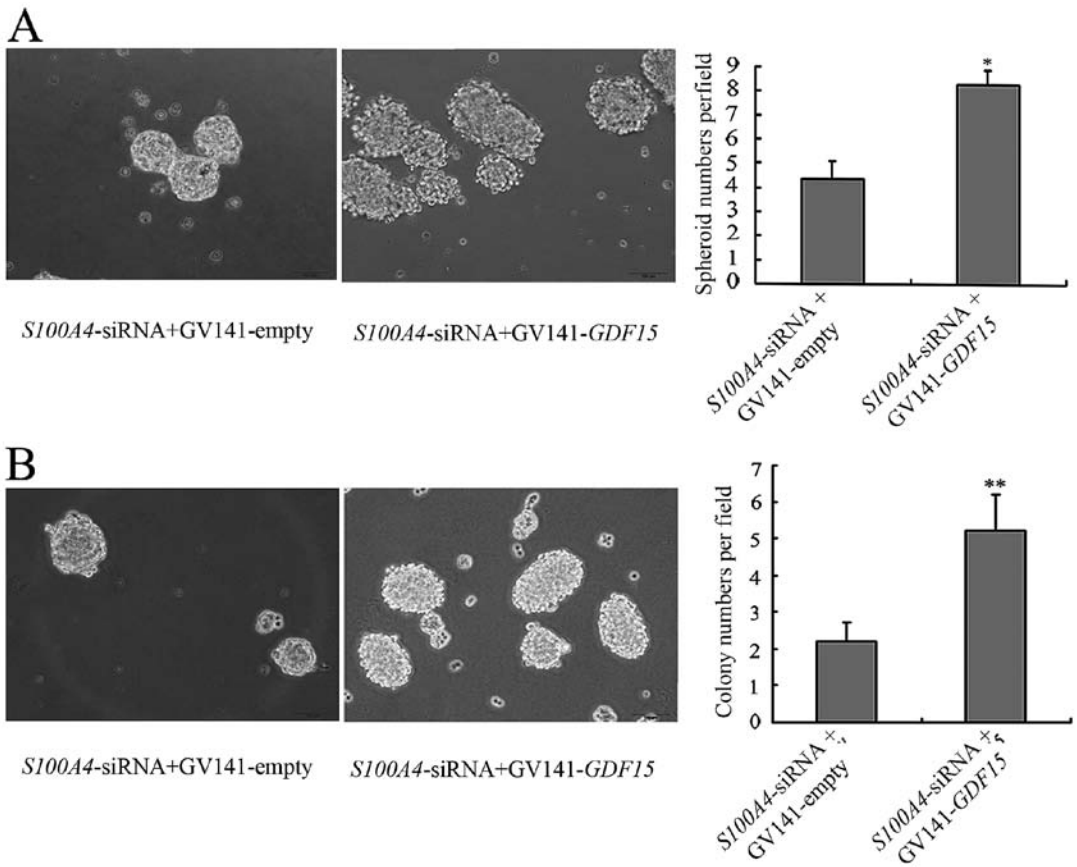

Figure 10. GV141-*GDF15* vector transfection reverses the effects of *S100A4* inhibition on the spheroid and soft-agar colony forming abilities of MGC803 cells. (A) Detection of spheroid forming ability: representative images of spheroids formed by MGC803/*S100A4*-siRNA+GV141-empty and MGC803/*S100A4*-siRNA+GV141-*GDF15* cells (left, magnification, x20). Bar graph (right) represents the mean number of spheroids from five randomly selected fields under the microscope, and error bars represent SD, *P<0.05. (B) Detection of colony forming ability: representative images of colonies formed by MGC803/*S100A4*-siRNA+GV141-empty and MGC803/*S100A4*-siRNA+GV141-*GDF15* cells (left, magnification, x20). Bar graph (right) represents the mean number of colonies from five randomly selected fields under the microscope, and error bars represent SD, **P<0.01. All the results were obtained from three repeat experiments.

significantly more spheroids and colonies were formed by MGC803/*S100A4*-siRNA+GV14-*GDF15* cells, indicating that *GDF15* mediates the effects of *S100A4* on the CSC-like properties of MGC803 cells (Fig. 10).

Discussion

Many studies have shown *S100A4* overexpression in various human cancers, such as hepatocellular, clear cell renal cell

and gastric cancers, and that it is closely related to metastasis and poor patient prognosis (15-17). Previously, our group demonstrated that reducing *S100A4* expression altered cell proliferation, apoptosis, migration and anoikis in BGC823 cells *in vitro*, and inhibited xenograft tumor growth *in vivo* (8,18,19). This led us to suggest that *S100A4* influences key cellular processes associated with the progression of gastric cancer. To gain insight into the mechanisms underlying this process, we first performed cDNA microarray analysis of the global alterations in gene expression in MGC803 gastric cancer cells following siRNA-mediated *S100A4* inhibition. Among the total genes investigated, 179 DEGs (38 upregulated and 141 downregulated) were identified in *S100A4*-siRNA transfected MGC803 cells compared with those transfected with NC-siRNA treated cells. In recent years, studies have shown that *S100A4* inhibition leads to changes in the expression of many genes in various tumor cells. In a study of the mechanism by which *S100A4* gene influences the invasiveness of prostate cancer cells using a microarray containing 96 well-characterized metastatic genes, Saleem *et al* (20) found that many genes, including matrix metalloproteinase 9 (*MMP-9*) and its tissue inhibitor (*TIMP-1*), were highly responsive to *S100A4* gene suppression. Using metastasis-related gene mRNA microarrays, Huang *et al* (21) identified some significantly dysregulated genes after downregulation of *S100A4*, including three downregulated genes (*MMP-9, MMP-10* and *CDH11*) and one upregulated gene (*TIMP-4*) in human colorectal cancer cells. Ochiya *et al* (22) reported that RNAi-mediated *S100A4* knockdown in mouse endothelial MSS31 cells markedly suppressed *in vitro* capillary-like tube formation in the early stages after treatment. Furthermore, this effect was found to be associated with down- and upregulation of the expression of some pro-angiogenic (*aqp1, fgf18, retn, map3k5, thy1, foxo6, hs6st1* and *mmp-3*) and anti-angiogenic (*cdknla, thbs1* and *spry4*) genes. These results indicated that *S100A4* influences the expression of many downstream genes in different kinds of cells. To the best of our knowledge, this study is the first to investigate the DEG profile downstream of *S100A4* in gastric cancer cells. The results provide important and extensive information for the clarification of the mechanism by which *S100A4* influences the progression of gastric cancer.

We undertook further bioinformatics analysis of the 179 DEGs to investigate the functional relevance of these genes. Pathway analysis showed the involvement of many of the 179 DEGs in 10 pathways, including the p53 signaling pathway, focal adhesion, ECM receptor interactions and others. GO annotation analysis revealed that DEGs were related to 10 types of molecular functions, including transferase activity, kinase activity, receptor binding and others. Nevertheless, a large number of the 179 DEGs were not associated with these pathways or molecular functions and their functions should not be ignored. In combination, our findings indicate that *S100A4* participates in a variety of pathways and influences many types of molecular functions by regulating downstream gene expression in gastric cancer cells.

Growth differentiation factor-15 (GDF15), also known as MIC-1, PTGFB and PLAB (23-25), is a divergent member of the TGF-β superfamily (26,27). Although normally undetectable under physiologic conditions in any tissues except the placenta (28), *GDF15* becomes highly upregulated under some pathological conditions, such as cancer, myocardial infarction and inflammation (29). *GDF15* has been shown to be a marker of mortality with high serum levels being a predictor of death, particularly due to cancer (30). Elevated circulating *GDF15* levels may correlate with poor clinical outcomes in endometrial cancer and can be used as a biomarker of the endometrial cancer phenotype, including the presence of lymph node metastasis and reduced survival (31). In addition, *GDF15* exerts an anti-apoptotic effect on oral squamous cell carcinoma cells *in vitro* (32). Tsui *et al* (33) demonstrated that *GDF15* overexpression induces cell proliferation, invasion, and tumorigenesis of PC-3 prostate carcinoma cells. All these results indicate that *GDF15* plays important roles in many types of cancers. Furthermore, in this study, *GDF15* was found to be one of the most notable DEGs, with downregulated expression after *S100A4* inhibition exceeding 5-fold identified in microarray analysis and 8-fold in the qRT-PCR analysis. These results indicate that *GDF15* is an important downstream gene of *S100A4* and is upregulated by it; consequently, we focused on *GDF15* in further research. First, we investigated the effects of *S100A4* on *GDF15* expression in gastric cancer cells. Previous report showed that S100A4 protein could interact with p53 protein and influence the expression of p53 target genes, such as *TSP-1* and *MDM2* in CSML-0 murine non-metastatic adenocarcinoma cells (34). Furthermore, cDNA microarray analysis in this study also showed differential expression of these genes after *S100A4* inhibition in gastric cancer MGC803 cells, which indicated that *S100A4* may also affect the expression of p53 target genes in MGC803 cells. Recently, it has been reported that *GDF15* is a direct target of p53 (35). ChIP analysis performed in this study to explore the mechanisms by which *S100A4* regulates *GDF15* expression revealed that S100A4 protein binds to the proximal promoter region of *GDF15*, which contains the p53 binding sites as reported (36). We speculated that S100A4 functions as a co-factor, interacting with p53 to regulate *GDF15* expression at the transcriptional level in MGC803 cells. In addition, the proximal promoter region of *GDF15* investigated in our ChIP analysis contains binding sites for other transcription factors such as Sp1 (37) and EGR-1 (38). Thus, it can be speculated that S100A4 may also affect the expression of *GDF15* by cooperating with Sp1, EGR-1 or other transcriptional factors. However, the underlying mechanism remains to be elucidated.

Next, we investigated the functional significance of *GDF15* in gastric cancer. It has been reported that *GDF15* is upregulated at the transcriptional level in tissues and cell lines of gastric cancers and *GDF15* increased the invasiveness of gastric cancer cells through regulation of urokinase plasminogen activator (39,40). In addition, studies have shown that serum levels of GDF15 and MMP-7 have diagnostic value for gastric cancers. The combination marker formed by GDF15, MMP-7 and miR-200c is indicative of adverse evolution in gastric cancer patients (41). However, the role of GDF15 in gastric cancer is far from clear. Recent studies show that *GDF15* can enhance the tumor-initiating and self-renewal potential of multiple myeloma cells (42). Therefore, we speculated that *GDF15* might affect CSC-like properties of gastric cancer cells. To investigate this, we analyzed the CSC-like properties of MGC803 cells transfected with a *GDF15* expression vector. We found that the numbers of spheroids and colonies

were increased significantly after *GDF15* expression vector transfection, indicating that *GDF15* promotes the CSC-like properties of MGC803 cells.

Our previous findings showed that IL-1β regulates spheroid and soft-agar colony forming abilities of MGC803 cells through *S100A4*, suggesting that *S100A4* might be involved in the regulation of CSC-like properties (unpublished data). In this study, we showed that *S100A4* inhibition led to decreased spheroid and soft-agar colony forming abilities of MGC803 cells, demonstrating that *S100A4* promotes the CSC-like properties of MGC803 cells.

Based on these findings, we speculated that *GDF15* might influence the effects of *S100A4* on the CSC-like properties in MGC803 gastric cancer cells. To test this hypothesis, we carried out rescue experiments by co-transfection of *S100A4*-siRNA with GV141-*GDF15* or GV141-empty into MGC803 cells. The results showed that GV141-*GDF15* vector transfection reversed the reduced spheroid and soft-agar colony forming abilities induced by *S100A4* inhibition. These findings suggest that, as a downstream effector, *GDF15* at least partly mediates *S100A4* regulation of CSC-like properties in MGC803 cells.

In conclusion, we conducted the first expression profile analysis of *S100A4* downstream genes in MGC803 gastric cancer cells, followed by experimental validation and functional analysis. Our results suggest that *S100A4* influences the expression of many genes in gastric cancer cells. S100A4 can bind to the *GDF15* promoter and may regulate its expression at the transcriptional level. We also provide experimental evidence suggesting that *GDF15* promotes the CSC-like properties of MGC803 gastric cancer cells, and that *S100A4* influences this effect by regulating *GDF15* expression. These data provide a novel overview of the effect of *S100A4* on the expression of downstream genes, and an insight into the mechanisms by which *S100A4* influences the CSC-like properties of MGC803 gastric cancer cells.

Acknowledgements

This study was supported by the National Natural Science Foundation of China; contract grant no. 81272717.

References

1. Boye K and Maelandsmo GM: S100A4 and metastasis: A small actor playing many roles. Am J Pathol 176: 528-535, 2010.
2. Natarajan J, Hunter K, Mutalik VS and Radhakrishnan R: Overexpression of S100A4 as a biomarker of metastasis and recurrence in oral squamous cell carcinoma. J Appl Oral Sci 22: 426-433, 2014.
3. Li H, Liu Z, Xu C, Chen Y, Zhang J, Cui B, Chen X, An G, She X, Liu H, *et al*: Overexpression of S100A4 is closely associated with the progression and prognosis of gastric cancer in young patients. Oncol Lett 5: 1485-1490, 2013.
4. Niu Y, Wang L, Cheng C, Du C, Lu X, Wang G and Liu J: Increased expressions of SATB1 and S100A4 are associated with poor prognosis in human colorectal carcinoma. APMIS 123: 93-101, 2015.
5. Zhang K, Zhang M, Zhao H, Yan B, Zhang D and Liang J: S100A4 regulates motility and invasiveness of human esophageal squamous cell carcinoma through modulating the AKT/Slug signal pathway. Dis Esophagus 25: 731-739, 2012.
6. Wang L, Wang X, Liang Y, Diao X and Chen Q: S100A4 promotes invasion and angiogenesis in breast cancer MDA-MB-231 cells by upregulating matrix metalloproteinase-13. Acta Biochim Pol 59: 593-598, 2012.
7. Che P, Yang Y, Han X, Hu M, Sellers JC, Londono-Joshi AI, Cai GQ, Buchsbaum DJ, Christein JD, Tang Q, *et al*: S100A4 promotes pancreatic cancer progression through a dual signaling pathway mediated by Src and focal adhesion kinase. Sci Rep 5: 8453, 2015.
8. Hua J, Chen D, Fu H, Zhang R, Shen W, Liu S, Sun K and Sun X: Short hairpin RNA-mediated inhibition of S100A4 promotes apoptosis and suppresses proliferation of BGC823 gastric cancer cells in vitro and in vivo. Cancer Lett 292: 41-47, 2010.
9. Clarke MF, Dick JE, Dirks PB, Eaves CJ, Jamieson CH, Jones DL, Visvader J, Weissman IL and Wahl GM: Cancer stem cells - perspectives on current status and future directions: AACR Workshop on cancer stem cells. Cancer Res 66: 9339-9344, 2006.
10. Takaishi S, Okumura T, Tu S, Wang SS, Shibata W, Vigneshwaran R, Gordon SA, Shimada Y and Wang TC: Identification of gastric cancer stem cells using the cell surface marker CD44. Stem Cells 27: 1006-1020, 2009.
11. Larzabal L, El-Nikhely N, Redrado M, Seeger W, Savai R and Calvo A: Differential effects of drugs targeting cancer stem cell (CSC) and non-CSC populations on lung primary tumors and metastasis. PLoS One 8: e79798, 2013.
12. Ping YF and Bian XW: Consice review: Contribution of cancer stem cells to neovascularization. Stem Cells 29: 888-894, 2011.
13. Liao J, Qian F, Tchabo N, Mhawech-Fauceglia P, Beck A, Qian Z, Wang X, Huss WJ, Lele SB, Morrison CD, *et al*: Ovarian cancer spheroid cells with stem cell-like properties contribute to tumor generation, metastasis and chemotherapy resistance through hypoxia-resistant metabolism. PLoS One 9: e84941, 2014.
14. Lo JF, Yu CC, Chiou SH, Huang CY, Jan CI, Lin SC, Liu CJ, Hu WY and Yu YH: The epithelial-mesenchymal transition mediator S100A4 maintains cancer-initiating cells in head and neck cancers. Cancer Res 71: 1912-1923, 2011.
15. Liu Z, Liu H, Pan H, Du Q and Liang J: Clinicopathological significance of S100A4 expression in human hepatocellular carcinoma. J Int Med Res 41: 457-462, 2013.
16. Yang H, Zhao K, Yu Q, Wang X, Song Y and Li R: Evaluation of plasma and tissue S100A4 protein and mRNA levels as potential markers of metastasis and prognosis in clear cell renal cell carcinoma. J Int Med Res 40: 475-485, 2012.
17. Wang YY, Ye ZY, Zhao ZS, Tao HQ and Chu YQ: High-level expression of S100A4 correlates with lymph node metastasis and poor prognosis in patients with gastric cancer. Ann Surg Oncol 17: 89-97, 2010.
18. Shen W, Chen D, Fu H, Liu S, Sun K and Sun X: S100A4 protects gastric cancer cells from anoikis through regulation of αv and α5 integrin. Cancer Sci 102: 1014-1018, 2011.
19. Chen D, Zhang R, Shen W, Fu H, Liu S, Sun K and Sun X: RPS12-specific shRNA inhibits the proliferation, migration of BGC823 gastric cancer cells with S100A4 as a downstream effector. Int J Oncol 42: 1763-1769, 2013.
20. Saleem M, Kweon MH, Johnson JJ, Adhami VM, Elcheva I, Khan N, Bin Hafeez B, Bhat KM, Sarfaraz S, Reagan-Shaw S, *et al*: S100A4 accelerates tumorigenesis and invasion of human prostate cancer through the transcriptional regulation of matrix metalloproteinase 9. Proc Natl Acad Sci USA 103: 14825-14830, 2006.
21. Huang L, Xu Y, Cai G, Guan Z and Cai S: Downregulation of S100A4 expression by RNA interference suppresses cell growth and invasion in human colorectal cancer cells. Oncol Rep 27: 917-922, 2012.
22. Ochiya T, Takenaga K and Endo H: Silencing of S100A4, a metastasis-associated protein, in endothelial cells inhibits tumor angiogenesis and growth. Angiogenesis 17: 17-26, 2014.
23. Bootcov MR, Bauskin AR, Valenzuela SM, Moore AG, Bansal M, He XY, Zhang HP, Donnellan M, Mahler S, Pryor K, *et al*: MIC-1, a novel macrophage inhibitory cytokine, is a divergent member of the TGF-beta superfamily. Proc Natl Acad Sci USA 94: 11514-11519, 1997.
24. Li PX, Wong J, Ayed A, Ngo D, Brade AM, Arrowsmith C, Austin RC and Klamut HJ: Placental transforming growth factor-beta is a downstream mediator of the growth arrest and apoptotic response of tumor cells to DNA damage and p53 overexpression. J Biol Chem 275: 20127-20135, 2000.
25. Hromas R, Hufford M, Sutton J, Xu D, Li Y and Lu L: PLAB, a novel placental bone morphogenetic protein. Biochim Biophys Acta 1354: 40-44, 1997.
26. Bauskin AR, Brown DA, Junankar S, Rasiah KK, Eggleton S, Hunter M, Liu T, Smith D, Kuffner T, Pankhurst GJ, *et al*: The propeptide mediates formation of stromal stores of PROMIC-1: Role in determining prostate cancer outcome. Cancer Res 65: 2330-2336, 2005.

27. Welsh JB, Sapinoso LM, Kern SG, Brown DA, Liu T, Bauskin AR, Ward RL, Hawkins NJ, Quinn DI, Russell PJ, *et al*: Large-scale delineation of secreted protein biomarkers overexpressed in cancer tissue and serum. Proc Natl Acad Sci USA 100: 3410-3415, 2003.
28. Paralkar VM, Vail AL, Grasser WA, Brown TA, Xu H, Vukicevic S, Ke HZ, Qi H, Owen TA and Thompson DD: Cloning and characterization of a novel member of the transforming growth factor-beta/bone morphogenetic protein family. J Biol Chem 273: 13760-13767, 1998.
29. Yin T, Cho SJ and Chen X: RNPC1, an RNA-binding protein and a p53 target, regulates macrophage inhibitory cytokine-1 (MIC-1) expression through mRNA stability. J Biol Chem 288: 23680-23686, 2013.
30. Wiklund FE, Bennet AM, Magnusson PK, Eriksson UK, Lindmark F, Wu L, Yaghoutyfam N, Marquis CP, Stattin P, Pedersen NL, *et al*: Macrophage inhibitory cytokine-1 (MIC-1/GDF15): A new marker of all-cause mortality. Aging Cell 9: 1057-1064, 2010.
31. Staff AC, Trovik J, Eriksson AG, Wik E, Wollert KC, Kempf T and Salvesen HB: Elevated plasma growth differentiation factor-15 correlates with lymph node metastases and poor survival in endometrial cancer. Clin Cancer Res 17: 4825-4833, 2011.
32. Schiegnitz E, Kämmerer PW, Koch FP, Krüger M, Berres M and Al-Nawas B: GDF 15 as an anti-apoptotic, diagnostic and prognostic marker in oral squamous cell carcinoma. Oral Oncol 48: 608-614, 2012.
33. Tsui KH, Chang YL, Feng TH, Chung LC, Lee TY, Chang PL and Juang HH: Growth differentiation factor-15 upregulates interleukin-6 to promote tumorigenesis of prostate carcinoma PC-3 cells. J Mol Endocrinol 49: 153-163, 2012.
34. Grigorian M, Andresen S, Tulchinsky E, Kriajevska M, Carlberg C, Kruse C, Cohn M, Ambartsumian N, Christensen A, Selivanova G, *et al*: Tumor suppressor p53 protein is a new target for the metastasis-associated Mts1/S100A4 protein: Functional consequences of their interaction. J Biol Chem 276: 22699-22708, 2001.
35. Tan M, Wang Y, Guan K and Sun Y: PTGF-beta, a type beta transforming growth factor (TGF-beta) superfamily member, is a p53 target gene that inhibits tumor cell growth via TGF-beta signaling pathway. Proc Natl Acad Sci USA 97: 109-114, 2000.
36. Osada M, Park HL, Park MJ, Liu JW, Wu G, Trink B and Sidransky D: A p53-type response element in the GDF15 promoter confers high specificity for p53 activation. Biochem Biophys Res Commun 354: 913-918, 2007.
37. Baek SJ, Horowitz JM and Eling TE: Molecular cloning and characterization of human nonsteroidal anti-inflammatory drug-activated gene promoter. Basal transcription is mediated by Sp1 and Sp3. J Biol Chem 276: 33384-33392, 2001.
38. Baek SJ, Kim JS, Moore SM, Lee SH, Martinez J and Eling TE: Cyclooxygenase inhibitors induce the expression of the tumor suppressor gene EGR-1, which results in the up-regulation of NAG-1, an antitumorigenic protein. Mol Pharmacol 67: 356-364, 2005.
39. Lee DH, Yang Y, Lee SJ, Kim KY, Koo TH, Shin SM, Song KS, Lee YH, Kim YJ, Lee JJ, *et al*: Macrophage inhibitory cytokine-1 induces the invasiveness of gastric cancer cells by up-regulating the urokinase-type plasminogen activator system. Cancer Res 63: 4648-4655, 2003.
40. Baek KE, Yoon SR, Kim JT, Kim KS, Kang SH, Yang Y, Lim JS, Choi I, Nam MS, Yoon M, *et al*: Upregulation and secretion of macrophage inhibitory cytokine-1 (MIC-1) in gastric cancers. Clin Chim Acta 401: 128-133, 2009.
41. Blanco-Calvo M, Tarrío N, Reboredo M, Haz-Conde M, García J, Quindós M, Figueroa A, Antón-Aparicio L, Calvo L and Valladares-Ayerbes M: Circulating levels of GDF15, MMP7 and miR-200c as a poor prognostic signature in gastric cancer. Future Oncol 10: 1187-1202, 2014.
42. Tanno T, Lim Y, Wang Q, Chesi M, Bergsagel PL, Matthews G, Johnstone RW, Ghosh N, Borrello I, Huff CA, *et al*: Growth differentiating factor 15 enhances the tumor-initiating and self-renewal potential of multiple myeloma cells. Blood 123: 725-733, 2014.